QUARTERLY OF APPLIED MATHEMATICS

VOLUME LV MARCH · 1997 NUMBER 1

MARCH 1997, PAGES 1–22

SLOW OSCILLATORY STOKES FLOW

BY

S. H. SMITH

Department of Mathematics, University of Toronto, Toronto, Ontario, Canada

Abstract. Two transient problems in slow viscous flow are considered where the corresponding steady-state behaviour leads to the paradoxical results of Stokes and Jeffery. First, the oscillatory flow past a circular cylinder is investigated when the frequency λ tends to zero, where an outer domain of size $O(\lambda^{-1/2})$ is required to ensure that the velocity conditions at infinity are satisfied. The flow close to the cylinder is quasi-steady except for a time of length $O(1)$ about the time of separation; most of the action takes place in the outer domain where the dominant transient behaviour extends over a time that is $O[\{\ln(\lambda^{-1})\}^{-1}]$ of a complete cycle.

The situation considered to illustrate the Jeffery paradox is the oscillatory flow due to a rotlet outside a circular cylinder. Here the outer region has two domains of size $O(\lambda^{-1/2})$ and $O[\{\lambda \ln(\lambda^{-1})\}^{-1}]$; in each domain there is continuous change for all time. The basic effect of the reversal in the direction of the rotlet requires more than a complete cycle to be noticed throughout the fluid.

1. Introduction. When an attempt is made to describe the slow viscous flow past a circular cylinder through solving the biharmonic equation, the correct behaviour at large distances cannot be gained; instead of the required finite velocity of a uniform stream, there is logarithmic growth. This is the well-known paradox first detected by Stokes [1]. However, when the convective forces are partially included in the approximation of Oseen [2], the anomalous behaviour is removed; since then, the concepts of singular perturbation theory presented by Kaplun and Lagerstrom [3], and Proudman and Pearson [4] have completed our understanding of the situation.

Similarly, Jeffery [5] discovered that when two equal circular cylinders rotate with equal but opposite angular velocities, the solution of the biharmonic equation indicates a uniform stream at large distances, rather than zero velocity. The resolution of this paradox also required understanding Jeffery's expression to be an inner solution, requiring an outer domain to complete the description.* Analytically, this implies considering the full Navier-Stokes equations, which is far from straightforward. In fact, even for the

Received September 17, 1993.

1991 *Mathematics Subject Classification.* Primary 76D07.

**Note added in proof.* The recent paper by Watson (The rotation of two circular cylinders in a viscous fluid, Mathematika 42 (1995) 105–126) has clarified this point.

Stokes' paradox the full solution of the linear Oseen equation for the circular cylinder is quite complex (cf. Tomotika and Aoi, [6]). The simplest model that displays the Jeffery paradox is that with a rotlet outside a circular cylinder—see Dorrepaal, O'Neill, and Ranger [7].

The intent of the present paper is to consider each of these behaviours from a different perspective. We investigate the time-dependent motion for both situations when the forcing term is oscillatory, but has small magnitude, and then consider the limiting case as the frequency of oscillation tends to zero. It is assumed throughout that the nonlinear inertial terms can be neglected so that the transient Stokes flow equations are appropriate. When these equations are solved for sufficiently simple geometries it is seen that the correct velocity conditions can be satisfied for all frequencies $\lambda > 0$; however, an outer domain is required as $\lambda \to 0$.

For the Stokes' problem, with an external forcing, it is seen in Sec. 2 that the outer domain is at distances $O(\lambda^{-1/2})$ from the cylinder, and the basic changes that take place in the fluid are during times t such that $\lambda t = \frac{1}{2}\pi + O[\{\ln(\lambda^{-1})\}^{-1}]$—around the time at which the direction of the uniform stream is reversed; during this period there is separation, plus the creation and then destruction of a free eddy. The flow in the inner region at finite distances from the cylinder is effectively quasi-steady with the classical biharmonic function solution dominating except for the time band of width $O(1)$ around the time of separation within this domain. The transition in the behaviour occupies a time whose length is only $O(\lambda)$ of the cycle of the oscillation. Consequently, the singular perturbation characteristics have two separate features: the existence of an outer domain where there is a relatively smooth change for all times t, and also the existence of a very small segment of the complete cycle during which change takes place in the inner domain.

For the Jeffery problem, where the force is locally generated, we find in Sec. 3 that there are two distinct outer domains at distances $O(\lambda^{-1/2})$ and $O[\{\lambda \ln(\lambda^{-1})\}^{-1}]$, and there is a continuous change in the behaviour throughout the cycle in these domains. The behaviour in the inner domain is quasi-steady, as in the Stokes problem.

Finally, a bounded flow which emphasizes very clearly the rapid transition around the time of the flow reversal is considered briefly in Sec. 4.

There has only been a limited discussion on the nature of oscillatory Stokes flows, even though the motion due to a sphere oscillation in viscous fluid was actually solved by Stokes [1] in his original paper. In fact, the nature of the streamlines for this situation was presented only recently by Pozrikidis [8]: he developed solutions numerically using the boundary integral method for a number of different axially symmetric geometries, indicating many interesting phenomena. Although the frequency of oscillations in his solutions was always finite, his results do suggest the possibility of fairly rapid transitions taking place, and it is this aspect that is highlighted by the asymptotic solutions presented here.

A survey of the background on transient Stokes flows is given in a chapter of the recent monograph by Kim and Karrila [9]. Once the results have been developed it can be seen that they have a greater applicability than just for oscillatory flows. When a general external force changes slowly in time, Basset [10] showed how the basically quasi-steady flow past a body is adjusted through the addition of a memory term, and his approach

is relevant for slow oscillations—except, that is, for times close to a change in direction. The major results here concern the adjustments that do take place around the transition and, when they are seen as describing the manner by which one quasi-steady motion is transformed into another through a change in direction, they can be applied to more general transient motions. In this regard the essential conclusions of Sec. 2 for two-dimensional flows are that the transition takes place over a large domain of the fluid, but close to the body takes a length of time after separation that is independent of the rate at which the external force is changing. However, from Sec. 3, it follows that when the transient force is local then there is never a quasi-steady behaviour at large distances.

In a two-dimensional polar coordinate system (r, θ) with length scale a, velocity scale U, and time scale $a^2\nu^{-1}$, we introduce a stream function $Ua\psi$ and vorticity $Ua^{-1}\omega$; here we have absorbed the coefficient of viscosity into the definition of the time. The Navier-Stokes equations are then

$$\omega_t - \frac{R}{r}\frac{\partial(\psi,\omega)}{\partial(r,\theta)} = \nabla^2\omega, \qquad \omega = \nabla^2\psi \tag{1}$$

for Reynolds number $R = Ua\nu^{-1}$. When we assume R to be small the time-dependent Stokes equation follows; further, when the motion is oscillatory with frequency of oscillation λ, writing

$$\psi(r,\theta,t) = \mathrm{Re}\{\Psi(r,\theta)e^{i\lambda t}\}, \qquad \omega(r,\theta,t) = \mathrm{Re}\{\Omega(r,\theta)e^{i\lambda t}\} \tag{2}$$

leads to the governing equation for slow oscillatory flow as

$$\nabla^2\Omega = i\lambda\Omega \quad \text{with} \quad \Omega = \nabla^2\Psi. \tag{3}$$

There are the two non-dimensional parameters R and λ, and so care could be necessary when different limits are taken for λ once R has been set as small. However, changing the value of λ implies changing the time scale, and so the main precaution is to ensure that rapid oscillations do not lead to large gradients in the nonlinear Jacobian of (1).

2. Oscillatory flow past a circular cylinder. When there is just an oscillatory streaming flow in the x-direction, the corresponding stream function is $\psi = r\sin\theta\cos\lambda t$. Consequently, when this is the far field flow in the presence of the circular cylinder $r = 1$, the mathematics is made much simpler by writing

$$\Psi(r,\theta) = F(r)\sin\theta, \qquad \Omega(r,\theta) = G(r)\sin\theta \tag{4}$$

for the governing ordinary differential equation

$$G'' + r^{-1}G' - r^{-2}G = i\lambda G \quad \text{with} \quad G = F'' + r^{-1}F' - r^{-2}F; \tag{5}$$

the boundary conditions require $F = F' = 0$, plus $F \cong r$ as $r \to \infty$. The solution to this problem is entirely straightforward and shows

$$F(r) = r - \frac{1}{r} - \frac{2}{r}\frac{K_1(\sigma)}{\sigma K_0(\sigma)} + \frac{2K_1(\sigma r)}{\sigma K_0(\sigma)} \quad \text{with} \quad \sigma = (i\lambda)^{1/2}. \tag{6}$$

When we introduce the Kelvin functions, $\ker_n(z)$ and $\mathrm{kei}_n(z)$, by

$$K_n(ze^{i\pi/4}) = e^{ni\pi/2}\{\ker_n(z) + i\,\mathrm{kei}_n(z)\}$$

(see Abramowitz and Stegun [11]), then (6) can be written as

$$\begin{aligned} F(r) = r - \frac{1}{r} &- \frac{\sqrt{2}}{\Delta\kappa r}[\ker_0(\kappa)\{\ker_1(\kappa) - \mathrm{kei}_1(\kappa)\} + \mathrm{kei}_0(\kappa)\{\ker_1(\kappa) + \mathrm{kei}_1(\kappa)\}] \\ &+ \frac{\sqrt{2}}{\Delta\kappa}[\ker_0(\kappa)\{\ker_1(\kappa r) - \mathrm{kei}_1(\kappa r)\} + \mathrm{kei}_0(\kappa)\{\ker_1(\kappa r) + \mathrm{kei}_1(\kappa r)\}] \\ &- \frac{\sqrt{2}i}{\Delta\kappa r}[\ker_0(\kappa)\{\ker_1(\kappa) + \mathrm{kei}_1(\kappa)\} + \mathrm{kei}_0(\kappa)\{\ker_1(\kappa) - \mathrm{kei}_1(\kappa)\}] \\ &+ \frac{\sqrt{2}i}{\Delta\kappa}[\ker_0(\kappa)\{\ker_1(\kappa r) + \mathrm{kei}_1(\kappa r)\} - \mathrm{kei}_0(\kappa)\{\ker_1(\kappa r) - \mathrm{kei}_1(\kappa r)\}] \end{aligned} \tag{7}$$

where $\Delta = \ker_0^2(\kappa) + \mathrm{kei}_0^2(\kappa)$ and $\kappa = \lambda^{1/2}$. Further, from (5) and (6) it is found that

$$G(r) = \frac{2\sigma K_1(\sigma r)}{K_0(\sigma)},$$

and when the real part of $Ge^{i\lambda t}$ is taken we have

$$\begin{aligned} \omega = (2\kappa)^{1/2}\Delta^{-1}U\sin\theta[&\{\mathrm{kei}_0(\kappa)g_1(r) - \ker_0(\kappa)g_2(r)\}\cos\lambda t \\ &- \{\mathrm{kei}_0(\kappa)g_2(r) + \ker_0(\kappa)g_1(r)\}\sin\lambda t], \end{aligned} \tag{8}$$

where $g_1(r) = \ker_1(\kappa r) - \mathrm{kei}_1(\kappa r)$, $g_2(r) = \ker_1(\kappa r) + \mathrm{kei}_1(\kappa r)$. This is the formal solution, and the flow properties can be obtained from an analysis of (7) and (8). Professor Howard Stone has constructed a vector invariant form for the velocity and vorticity fields for this problem, which is presented as an appendix to the present paper; this approach has a much greater elegance than the stream function development described above, and the author wishes to acknowledge with gratitude his contribution.

Before developing the asymptotic solutions that follow from (7) as $\lambda \to 0$ we consider the particular case when $\lambda = 0.01$. A numerical investigation indicates a number of different stages in the half-cycle where $0 \leq 0.01t \leq \pi$; for $\pi \leq 0.01t \leq 2\pi$ the pattern is repeated with only the change in direction. The description is commenced at the time $t = 0$ where the velocity at large distances has its maximum magnitude. As t increases, the velocities decrease, but the basic topology of the streamlines is unchanged (Fig. 1(a)).

However, when $0.01t \cong 0.4058\pi$ the vorticity on the boundary has fallen to zero and there is separation from the cylinder; subsequently, an attached eddy grows away from

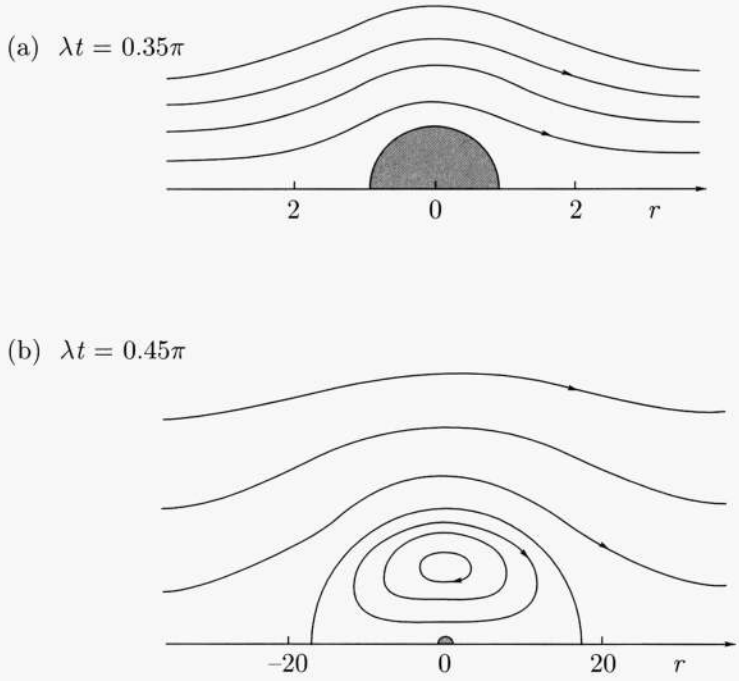

FIG. 1(i). Streamlines for the flow past a circular cylinder when $\lambda = 0.01$: (a) $\lambda t = 0.35\pi$; (b) $\lambda t = 0.45\pi$.

the surface with a stagnation point along the line $\theta = \frac{1}{2}\pi$. When $0.01t = \frac{1}{2}\pi$ the free stream velocity at infinity is zero, and following this reversal a second stagnation point develops on $\theta = \frac{1}{2}\pi$ at infinity and begins to move in; there is now a distinctive free eddy in the fluid, though at a fairly large distance from the cylinder (see Fig. 1(c) on p. 6). The two stagnation points move together quickly, before coalescing when $0.01t \cong 0.5135\pi$ at $r \cong 41.3$ as the free eddy collapses. When $0.01t = 0.52\pi$ the evidence that this eddy has existed at large distances is just the presence of an inflow of fluid (see Fig. 1(d) on p. 6), but locally the streamlines are effectively those shown in Fig. 1(a). At $0.01t = 0.6\pi$ the flow throughout the fluid is represented by Fig. 1(a). Although the eddy is present only during the time $\frac{1}{2}\pi < 0.01t < 0.5135\pi$ (that is, for approximately 1.35% of the half-cycle), it is clear that its role is crucial in the transition from the flow in one direction to the other.

In Table 1 (see p. 7) the time development of the vorticity ω, given by (8), is presented for different positions in the fluid. The steep gradient close to the cylinder is evident (notwithstanding the zero Reynolds number), except around the separation time; the velocity derivative is zero when $0.01t = 0.3960\pi$ just before separation takes place. Although no direct connection can be established, it can be observed that the vorticity gradients are small where and when the free eddy collapses in the fluid.

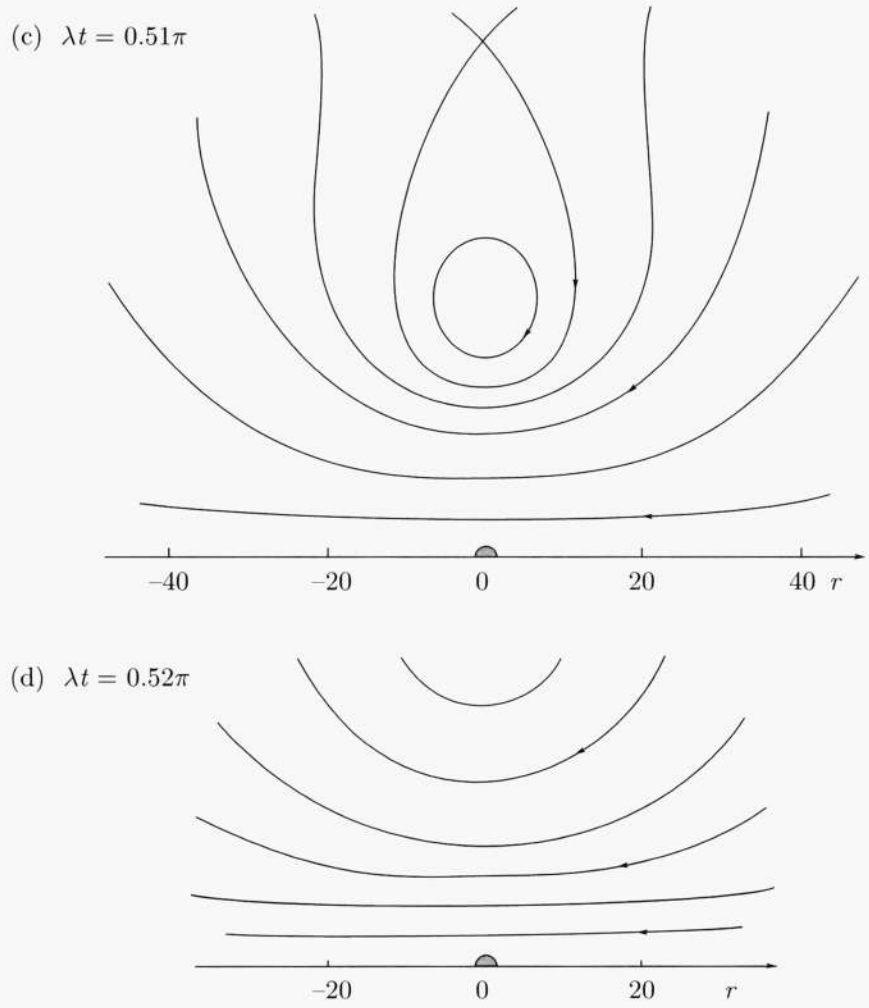

FIG. 1(ii). Streamlines for the flow past a circular cylinder when $\lambda = 0.01$: (c) $\lambda t = 0.51\pi$; (d) $\lambda t = 0.52\pi$.

Further numerical computations indicate that the structure of the transition described above is present for all small or moderate values of λ. For $\lambda = 1$, for example, separation takes place when $t \cong 0.317\pi$, and the free eddy exists for $\frac{1}{2}\pi < t < 0.524\pi$, dying out at $r \cong 5.33$. Separation always takes place from the surface of the cylinder during the decelerating phase of the flow (cf. Pozrikidis [8] for the equivalent result for the sphere) with the time of separation for different values of λ given by

$$\tan \lambda t = \frac{\mathrm{kei}_0(\kappa)\{\mathrm{ker}_1(\kappa) - \mathrm{kei}_1(\kappa)\} - \mathrm{ker}_0(\kappa)\{\mathrm{ker}_1(\kappa) + \mathrm{kei}_1(\kappa)\}}{\mathrm{kei}_0(\kappa)\{\mathrm{ker}_1(\kappa) + \mathrm{kei}_1(\kappa)\} + \mathrm{ker}_0(\kappa)\{\mathrm{ker}_1(\kappa) - \mathrm{kei}_1(\kappa)\}};$$

these are represented in Fig. 2.

We now turn to an asymptotic analysis of the stream function (6). Clearly, $F \cong r$ as $r \to \infty$ for all $\lambda > 0$, and so the free stream is definitely approached at large distances

TABLE 1. The values of the vorticity ω/U for points in the fluid on the line $\theta = \frac{1}{2}\pi$ at different times t in the cycle for the oscillatory flow past a circular cylinder when $\lambda = 0.01$, as calculated from (8).

r \ λt	0	0.25π	0.4π	0.41π	0.45π
1	34.251	16.833	0.649	-0.472	-4.977
2	17.093	8.808	0.862	0.307	-1.925
4	8.389	4.853	1.142	0.876	-0.198
6	5.368	3.507	1.270	1.105	0.433
12	2.060	1.882	1.208	1.152	0.914
18	0.843	1.073	0.902	0.883	0.798
24	0.280	0.582	0.583	0.579	0.559
30	0.027	0.258	0.330	0.332	0.338
36	-0.065	0.087	0.160	0.163	0.177
42	-0.082	0.004	0.058	0.062	0.074
48	-0.067	-0.027	0.006	0.009	0.018

r \ λt	0.5π	0.52π	0.6π	0.75π	π
1	-10.446	-12.576	-20.518	-31.605	-34.251
2	-4.647	-5.711	-9.701	-15.372	-17.093
4	-1.525	-2.049	-4.042	-7.010	-8.389
6	-0.409	-0.745	-2.048	-4.085	-5.368
12	0.601	0.470	-0.065	-1.032	-2.060
18	0.675	0.620	0.381	0.119	-0.843
24	0.522	0.503	0.410	0.171	-0.280
30	0.338	0.336	0.313	0.220	-0.027
36	0.189	0.193	0.200	0.180	0.065
42	0.088	0.093	0.109	0.120	0.082
48	0.028	0.033	0.048	0.067	0.067

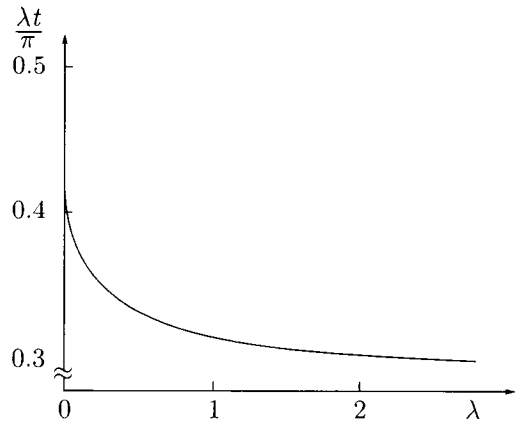

FIG. 2. Time of separation from the surface of the circular cylinder for different values of the frequency λ.

from the cylinder; there is no Stokes paradox for the solution of the linear oscillatory flow equations (5) as long as λ is strictly greater than zero. However, when r is finite and $0 < \lambda \ll 1$, it is found from (4), (6) that

$$\Psi = -\frac{(2r\ln r - r + r^{-1})\sin\theta}{\ln(i\lambda) - 2\ln 2 + 2\gamma} + O(\lambda), \quad r = O(1); \tag{9}$$

the numerator is the well-known biharmonic function found by Stokes which has the singular behaviour as $r \to \infty$. When the real and imaginary parts are taken, we have

$$\psi = \frac{4\alpha\cos\lambda t - 2\pi\sin\lambda t}{4\alpha^2 + \pi^2}(2r\ln r - r + r^{-1})\sin\theta + O(\lambda), \quad r = O(1), \tag{10}$$

where

$$\alpha = \ln(\lambda^{-1}) - 2\ln 2 + 2\gamma.$$

Consequently, the motion where $r = O(1)$ is quasi-steady for all times t except in the narrow band for λt around the time $t = t_s$ where $\lambda t_s \cong \frac{1}{2}\pi - \frac{1}{2}\pi\alpha^{-1}$; this is the time when the flow separates from the cylinder. (The presence of logarithmic terms in λ indicates that there are two types of limiting behaviour—where the error is small as λ and where it is small as α^{-1}—and care must be taken to distinguish between them when particular numerical examples are considered because of the slow divergence of $\ln\lambda$. For example, the time t_s is given by $\lambda t_s = \frac{1}{2}\pi$ when $\lambda \to 0$, even though when λ is as small as 10^{-6} we have $\lambda t_s \cong 0.465\pi$ only; nevertheless, the transition at finite distances from the cylinder does take place during a time-band for λt around λt_s which is $O(10^{-6})$ in width, and so it will be numerically indistinguishable from $\lambda t \cong 0.465\pi$.)

The $O(\lambda)$ error term in (9) has been calculated, and is seen to give the extra contribution

$$\tfrac{1}{8}\lambda(r^3 - 2r + r^{-1})\sin\theta\sin\lambda t \tag{11}$$

towards $\psi(r,\theta,t)$ as given by (10); the expression (11) represents the parabolic flow past a circular cylinder. After separation at $t = t_s$ an attached eddy is formed around the cylinder and then grows in size; stagnation points are present on $|\theta| = \frac{1}{2}\pi$. Once $t - t_s \gg 1$ the flow reversal is complete in the neighbourhood of the cylinder because of the separation, even though the flow at infinity is still in the original direction with $\lambda t < \frac{1}{2}\pi$. The rate at which this local reversal takes place is independent of λ for sufficiently small values. The general flow for $\lambda t_s < \lambda t < \frac{1}{2}\pi$ is well illustrated by Fig. 1(c).

The calculations so far have displayed the inner solution at finite distances from the cylinder, and there is clearly a distinguished limit when

$$\rho = \lambda^{\frac{1}{2}} r = O(1) \quad \text{for } 0 < \lambda \ll 1,$$

to define the outer domain. Here, it can be seen from (7) that

$$\lambda^{\frac{1}{2}} F = \left[\rho - \frac{8\pi}{4\alpha^2 + \pi^2}\frac{1}{\rho} + \frac{4\sqrt{2}}{4\alpha^2 + \pi^2}\{(2\alpha - \pi)\,\mathrm{ker}_1(\rho) - (2\alpha + \pi)\,\mathrm{kei}_1(\rho)\}\right]$$
$$+ i\left[-\frac{16\alpha}{4\alpha^2 + \pi^2}\frac{1}{\rho} + \frac{4\sqrt{2}}{4\alpha^2 + \pi^2}\{(2\alpha + \pi)\,\mathrm{ker}_1(\rho) + (2\alpha - \pi)\,\mathrm{kei}_1(\rho)\}\right] + O(\lambda); \tag{12}$$

we have retained a number of terms in (12) to give a precise understanding of the error involved, but when only the dominant terms for the real and imaginary parts of F are included as $\lambda \to 0$ it follows that the stream function $\psi(r, \theta, t)$ becomes

$$\lambda^{\frac{1}{2}}\psi \cong \left[\rho \cos \lambda t + \frac{2\sqrt{2}}{\alpha}\left\{\frac{\sqrt{2}}{\rho} + \ker_1(\rho) + \mathrm{kei}_1(\rho)\right\}\sin \lambda t\right]\sin\theta. \tag{13}$$

Hence, the dominant motion in the limiting case as $\lambda \to 0$ is just the uniform stream for $\rho = O(1)$ except, that is, for those times where $\lambda t = \frac{1}{2}\pi + O(\alpha^{-1})$. The boundary of the attached eddy formed on the surface of the cylinder at separation is $\psi = 0$, and this moves out continuously through the domain $\rho = O(1)$ for $t > t_s$, reaching infinity by $\lambda t = \frac{1}{2}\pi$; from a numerical analysis of (13) it is seen that the stagnation point within the eddy is then at $\rho \cong 2.045$. The second stagnation point, which is created at infinity when $\lambda t = \frac{1}{2}\pi$, moves inwards for $\lambda t > \frac{1}{2}\pi$, and coalesces with the initial stagnation point $\rho = \rho_c \cong 3.548$ when $t = t_c$ where $\lambda t_c \cong \frac{1}{2}\pi + 0.300\alpha^{-1}$. For $\frac{1}{2}\pi < \lambda t < \lambda t_c$ there is always the free eddy in the fluid with the characteristics of that found when $\lambda = 0.01$; it exists in the outer domain $\rho = O(1)$ only, and is depicted in Fig. 3.

For large values of ρ, the Kelvin functions are exponentially small, and so we can write

$$\lambda^{\frac{1}{2}}\psi \cong \left\{\left(\rho - \frac{8\pi}{4\alpha^2 + \pi^2}\frac{1}{\rho}\right)\cos \lambda t - \frac{16\alpha}{4\alpha^2 + \pi^2}\frac{\sin \lambda t}{\rho}\right\}\sin\theta, \quad \text{for } \rho \gg 1,$$

when $0 < \lambda \ll 1$ from (12). This expression is a combination of the uniform stream plus a weak dipole for all times; consequently, the streamlines at a large distance are displaced outwards (being equivalent to the inviscid flow past a circular cylinder with radius $O(\alpha^{-\frac{1}{2}})$) when the direction of the dipole is opposite to that of the stream, and inwards when the direction of the dipole is the same as that of the stream.

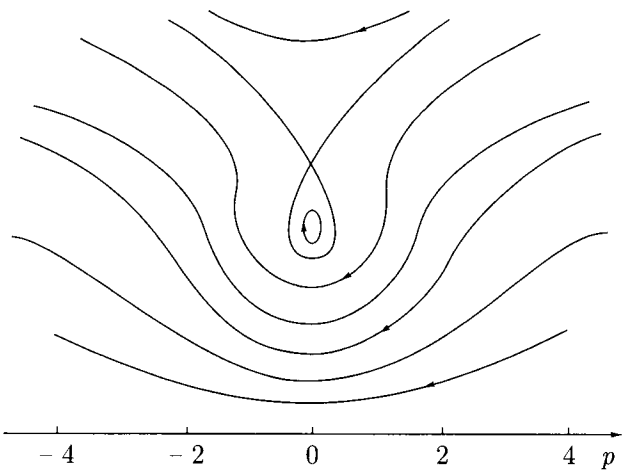

FIG. 3. Streamlines for the flow past a circular cylinder in the outer domain $\rho = O(1)$ for small frequencies λ when $\lambda t = \frac{1}{2}\pi + 0.28\alpha^{-1}$.

To summarize, there are the two basic stages within the transition process: firstly, the separation and growth of an attached eddy when $\lambda t < \frac{1}{2}\pi$ and, secondly, the development and subsequent collapse of the free eddy in the outer domain when $\lambda t > \frac{1}{2}\pi$. The qualitative structure of the flow presented in the particular case $\lambda = 0.01$ (and even seen for $\lambda = 1$) is still appropriate in the asymptotic case $\lambda \to 0$; however, the quantitative values are not particularly accurate in those situations where the error is as large as $O(\alpha^{-1})$.

3. Rotlet outside a circular cylinder. When a rotlet of constant strength is present outside a circular cylinder the solution of the biharmonic equation that represents the motion due to the rotlet locally, satisfying the no-slip conditions on the cylinder, does not show velocities that decay at a large distance—rather it shows a uniform stream whose direction is perpendicular to the line joining the rotlet to the centre of the cylinder. This was the result presented by Dorrepaal, O'Neill, and Ranger [7] to illustrate the Jeffery paradox.

We now consider the time-dependent case where the rotlet is positioned at $r = c$, $\theta = 0$ (with $c > 1$), and has the oscillatory strength $\cos \lambda t$. The equations (3) are appropriate, where Ψ and Ω are defined by (2) as before. In the neighbourhood of the rotlet $\Psi \cong \frac{1}{2}\ln(r^2 - 2cr\cos\theta + c^2)$, and when the equations (3) plus the conditions $\Psi = \Psi_r = 0$ on $r = 1$ are satisfied, it is found by straightforward Fourier series analysis that

$$\Psi = \frac{1}{2}\ln\left\{\frac{(r^2 - 2cr\cos\theta + c^2)c^2r^2}{c^2r^2 - 2cr\cos\theta + 1}\right\} - \frac{2}{\sigma}\sum_{n=1}^{\infty}\frac{\cos n\theta}{c^{n-1}K_{n-1}(\theta)}\left\{K_n(\sigma r) - \frac{K_n(\sigma)}{r^n}\right\}, \quad (14)$$

where $\sigma^2 = i\lambda$. The first term is the inviscid solution, found by the method of images, and gives the dominant behaviour $\Psi \cong \ln r$ as $r \to \infty$ for all $\lambda > 0$; the velocity does tend to zero at large distances. The vorticity on the cylinder can be found directly from (14), and is given by

$$(\Omega)_{r=1} = -\frac{4\sigma}{\pi}\sum_{n=1}^{\infty}\frac{K_n(\sigma)}{c^nK_{n-1}(\sigma)}\cos n\theta. \quad (15)$$

Here we find that there are three distinct domains to the flow when λ is small, and we investigate these in turn. An approximate numerical analysis of (14) has been made for the particular case $\lambda = 0.01$; however, there are difficulties of scale in presenting these results in full, and we extract local information where appropriate in the context of the asymptotic solution. We do note now, though, that the structure of the flow found when $\lambda = 0.01$ can be identified within the asymptotic analysis (as we saw for the simpler case in the previous section) even though the quantitative details do differ in places where the asymptotic solution has an error no smaller that $O(\alpha^{-1})$ as $\lambda \to 0$.

To begin, it can be shown for $r = O(1)$ that

$$\frac{K_n(\sigma r) - r^{-n}K_n(\sigma)}{\sigma K_{n-1}(\sigma)} \cong -\frac{r^2 - 1}{2r^n} \quad \text{as } \lambda \to 0 \quad (16)$$

for all n. The error in (16) is $O(\lambda)$ when $n = 3, 4, 5, \ldots$, and is $O\{\lambda \ln(\lambda^{-1})\}$ when $n = 2$: the largest error occurs when $n = 1$, where

$$\frac{K_1(\sigma r) - r^{-1}K_1(\sigma)}{\sigma K_0(\sigma)} = -\frac{r^2 - 1}{2r} + \frac{2r\ln r - r + r^{-1}}{2\alpha - i\pi} + O\{\lambda \ln(\lambda^{-1})\}, \tag{17}$$

with $\alpha = \ln(\lambda^{-1}) + 2\ln 2 - 2\gamma$ as before. When the right-hand side of (16) is substituted into (14), the series can be summed to show

$$\begin{aligned}\Psi =& \frac{1}{2}\ln\left\{\frac{(r^2 - 2cr\cos\theta + c^2)c^2r^2}{c^2r^2 - 2cr\cos\theta + 1}\right\} + \frac{(r^2 - 1)(cr\cos\theta - 1)}{c^2r^2 - 2cr\cos\theta + 1} \\ &+ \frac{2\alpha + i\pi}{c(4\alpha^2 + \pi^2)}(2r\ln r - r + r^{-1})\cos\theta + O\{\lambda\ln(\lambda^{-1})\}.\end{aligned} \tag{18}$$

The leading-order solution for Ψ as $\lambda \to 0$ is given by the first two terms of (18), and is just the steady-state solution found by Dorrepaal, O'Neill, and Ranger. The vorticity on the boundary which follows from (18) is given by

$$\frac{\pi}{8}(\Omega)_{r=1} = -\frac{c^2\cos 2\theta - 2c\cos\theta + 1}{(c^2 - 2c\cos\theta + 1)^2} + \frac{2(2\alpha + i\pi)}{c(4\alpha^2 + \pi^2)}\cos\theta + O\{\lambda\ln(\lambda^{-1})\}. \tag{19}$$

For the physical stream function $\psi(r, \theta, t)$ and vorticity $\omega(r, \theta, t)$ it is only during the times where $\lambda t = \frac{1}{2}\pi + O(\alpha^{-1})$ that the flow is not quasi-steady in the inner domain $r = O(1)$—in the beginning we are concerned with times in the half-cycle $0 \leq \lambda t < \pi$. Outside this time band the streamlines are equivalent to those presented from the steady-state flow; in Fig. 4(a) (see p. 12) when $c = 2$, there are separation points at the two particular values of $|\theta|$ with $|\theta_{s1}| \cong 24.3°$ and $|\theta_{s2}| \cong 114.3°$. (The value of c has no qualitative influence on the behaviour, and so we maintain the particular value $c = 2$ throughout this section.)

Shortly before $\lambda t = \frac{1}{2}\pi$ the cell containing the rotlet decreases in size as the separation points at $\pm\theta_{s1}$ move towards the axis $\theta = 0$; the cell breaks away from the cylinder when $\lambda t \cong (\frac{1}{2} - \frac{1}{4}\alpha^{-2})\pi$ for $\lambda \ll 1$, and continues to collapse; cf. Fig. 4(b). Shortly after $\lambda t = \frac{1}{2}\pi$ the direction of the rotlet has reversed with the streamlines now similar to those shown in Fig. 4(c); these diagrams correspond to the particular case $\lambda = 0.01$, where the cell breaks away when $0.01t \cong 0.4917\pi$. Subsequently, the stagnation point on $\theta = 0$ moves away to infinity, and the $\psi = 0$ streamline moves in from infinity along $\theta = 0$ to form the cell that encloses the rotlet. Also, separation takes places on $r = 1$ at $\theta = \pi$ for $\lambda t \cong (\frac{1}{2} + \frac{9}{4}\alpha^{-2})\pi$, and the quasi-steady flow as depicted in Fig. 4(a) comes to dominate again as the reversal in the flow direction is complete.

The position of the points of separation on the cylinder, as found from equating $(\omega)_{r=1}$ to zero, are shown in Fig. 5 (see p. 13) for $\lambda = 0.01$. From this graph it is seen that the position on the front portion is stable for much of the cycle, though that on the rear portion moves more continuously; this movement occupies more than one cycle. If we consider the separation that commences at $\theta = \pi$ when $0.01t \cong 0.8258\pi$, the points move around the rear portion of the cylinder, passing continuously through the steady-state position $|\theta_{s2}| \cong 114.3°$, accelerating through $\theta = \frac{1}{2}\pi$ when $0.01t = \frac{3}{2}\pi$, staying close to

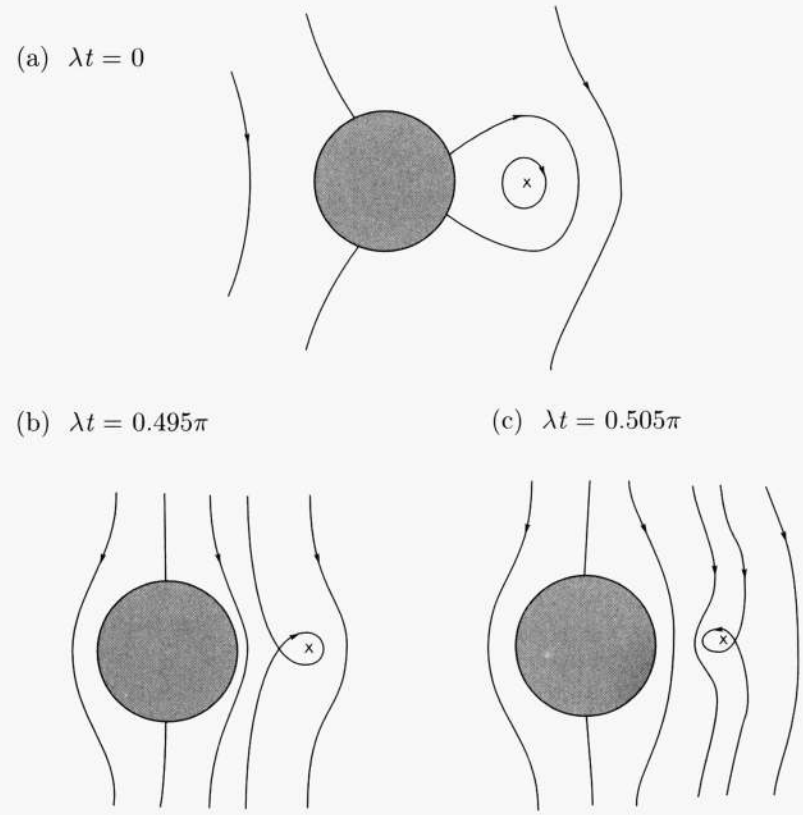

FIG. 4. Local streamlines for the flow due to a rotlet outside a circular cylinder when $c = 2$, $\lambda = 0.01$: (a) $\lambda t = 0$; (b) $\lambda t = 0.495\pi$; (c) $\lambda t = 0.505\pi$.

$|\theta_{s1}| \cong 24.3°$ for almost a complete half-cycle, before eventually moving rapidly to $\theta = 0$ by $0.01t = 2.4917\pi$. This pattern is repeated every half-cycle, with separation starting at $\theta = \pi$ when $0.01t = (0.8258+n)\pi$, and disappearing at $\theta = 0$ when $0.01t = (2.4917+n)\pi$, for all integers n.

The results for $\lambda = 0.01$ show a clear difference in the behaviour between the front and rear portions of the cylinder that is not immediately obvious from the asymptotic results. When λ is small, (19) shows that separation commences at $\theta = \pi$ when $\tan \lambda t = -(4\alpha^2 - 18\alpha + \pi^2)/(9\pi) + O\{\lambda \ln(\lambda^{-1})\}$, which indicates $\lambda t \cong (\frac{1}{2} + \frac{9}{4}\alpha^{-2})\pi$ as $\lambda \to 0$. The separation points move to the steady-state position $|\theta_{s2}|$ during a time that is $O(\alpha^2)$ where, formally, it remains for almost a complete half-cycle (although a very small value of λ is necessary for this to be recognizable); they then move to $|\theta_{s1}|$, staying there for almost a complete half-cycle before continuing on towards $\theta = 0$ where they vanish for t given by $\tan \lambda t = (4\alpha^2 + 2\alpha + \pi^2)/\pi + O\{\lambda \ln(\lambda^{-1})\}$, which indicates $\lambda t \cong (\frac{5}{2} - \frac{1}{4}\alpha^{-2})\pi$ as $\lambda \to 0$. Numerically, it is the steep slope of the first term for $(\Omega)_{r=1}$ (given by (19)) for θ around θ_{s1}, and the shallow slope for θ around θ_{s2}, that leads to the more rapid changes on the front portion indicated in Fig. 5.

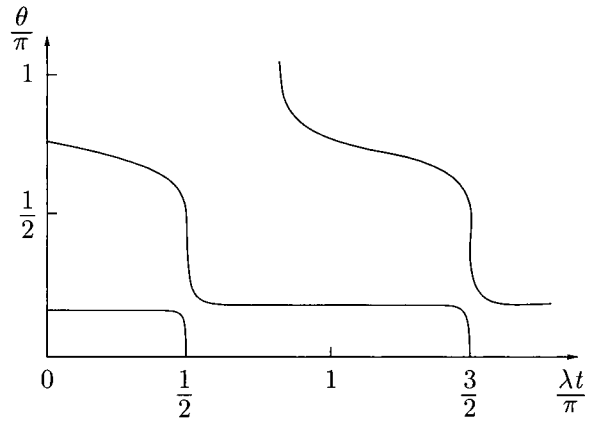

FIG. 5. Position of the separation points on the surface of a circular cylinder when there is a rotlet at $c = 2$, $\theta = 0$; the frequency is $\lambda = 0.01$.

As evident from the form of the solution (14), and by comparison with the behaviour described in the previous section, it is clear that there is an outer region when $\lambda \ll 1$ where ρ is finite, with $\rho = \lambda^{\frac{1}{2}} r$ as before. When $\rho = O(1)$,

$$\frac{K_n(\sigma r) - r^{-n} K_n(\sigma)}{\sigma K_{n-1}(\sigma)} = \begin{cases} O(\lambda^{\frac{1}{2}n-1}) & \text{for } n = 2, 3, 4, \ldots, \\ O[\lambda^{-\frac{1}{2}}\{\ln(\lambda^{-1})\}^{-1}] & \text{for } n = 1; \end{cases} \tag{20}$$

consequently, the $n = 1$ term dominates throughout this region, and when the precise form of the term is calculated we have

$$\Psi = \frac{8\sqrt{2}(2\alpha + i\pi)}{\pi c \lambda^{\frac{1}{2}}(4\alpha^2 + \pi^2)} \left[\{\mathrm{ker}_1(\rho) - \mathrm{kei}_1(\rho)\} + i \left\{ \frac{\sqrt{2}}{\rho} + \mathrm{ker}_1(\rho) + \mathrm{kei}_1(\rho) \right\} \right] \cos\theta + O(1), \quad \text{for } \rho = O(1). \tag{21}$$

An immediate observation is that the magnitude of Ψ is large compared to unity, and so dominates the contribution due to the rotlet itself; therefore, there must be a third (outermost) domain where $\rho \gg 1$ within which the expression given in (21) (where the square bracket is $O(\rho^{-1})$ as $\rho \to \infty$) does balance the $\ln r$ term representing the rotlet. Further, the strength of the rotlet must certainly be sufficiently small so that the basic linearisation throughout this work is still valid.

As a first step in the development of an understanding of the behaviour given by (21), it is seen that the only role of the imaginary part of the factor $(2\alpha + i\pi)$ is to give a phase shift of $O(\alpha^{-1})$ in the description that follows, and we find that this has a limited role on the basic flow. Hence, we investigate the streamlines at different times for

$$\psi \cong \frac{4\sqrt{2}}{\pi c \lambda^{\frac{1}{2}} \ln(\lambda^{-1})} \{\mathcal{R}(\rho) \cos \lambda t - \mathcal{S}(\rho) \sin \lambda t\} \cos \theta \tag{22}$$

where $\mathcal{R}(\rho) = \mathrm{ker}_1(\rho) - \mathrm{kei}_1(\rho)$ and $\mathcal{S}(\rho) = \sqrt{2}\rho^{-1} + \mathrm{ker}_1(\rho) + \mathrm{kei}_1(\rho)$. The expression in the brackets in (22) is independent of λ for finite ρ, and so the changes take place steadily throughout the cycle in this outer domain. In Fig. 6 we plot the graph that represents the position of the stagnation points on the axes $\theta = 0, \pi$ for different times t, as found from calculating where $\tan \lambda t = \mathcal{R}'/\mathcal{S}'$ from (22); we find that this helps to give an understanding of the flow structure. When $\lambda t = \frac{1}{2}\pi$, a stagnation point develops at $\rho = 0$ (corresponding to the reversal in direction of rotation for finite r), which leads to a bifurcation, and two separate points moving out symmetrically along each axis. They have reached $\rho \cong 0.810$ when $\lambda t = \pi$, and $\rho \cong 1.476$ when $\lambda t = \frac{3}{2}\pi$; at this time another stagnation point develops at $\rho = 0$, and this pattern continues to repeat itself with period π/λ. The stagnation point that starts at $\rho = 0$ when $\lambda t = \frac{1}{2}\pi$ has reached $\rho = 6.109$ when $\lambda t = 2\pi$; the speed is increasing. Now $\mathcal{R}(\rho)$ is oscillatory in ρ with exponentially small magnitude as ρ increases, and there are (formally) an infinite set of stagnation points according to (22). However, because the $\ln r \cos \lambda t$ term from the rotlet has been neglected in this representation, it can be expected that the domain of validity for (22) does not extend to values of ρ that are too large—an observation that is confirmed in the numerical computations for the particular case $\lambda = 0.01$. With this proviso, the streamline patterns that follow from (22) have just two configurations, one for $0 \leq \lambda t \leq \frac{1}{2}\pi$ and the other for $\frac{1}{2}\pi < \lambda t < \pi$, and these are drawn in Figs. 7(a), (b) respectively; there is a symmetry about $|\theta| = \frac{1}{2}\pi$ when $\rho = O(1)$. When we consider the matching between the inner solution (as given by (18)) where $r \to \infty$, and the outer solution (as given by (21)) where $\rho \to 0$, it is seen that the flow is dominated by the streaming motion which is represented by different combinations of the $r \cos \theta$ and $r \ln r \cos \theta$ terms at different times; this behaviour is observed in Figs. 4 and 7.

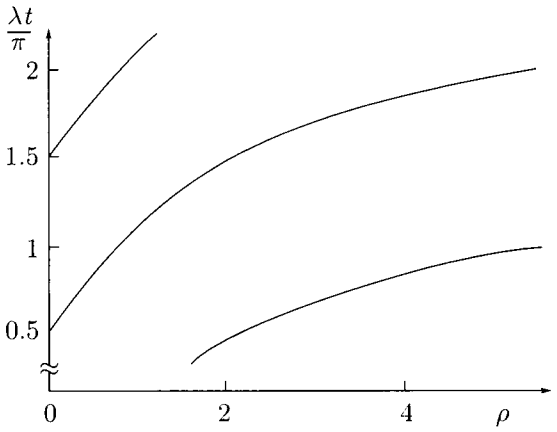

FIG. 6. Position of the stagnation points on the axes $\theta = 0, \pi$ in the domain $\rho = O(1)$ for small frequencies λ.

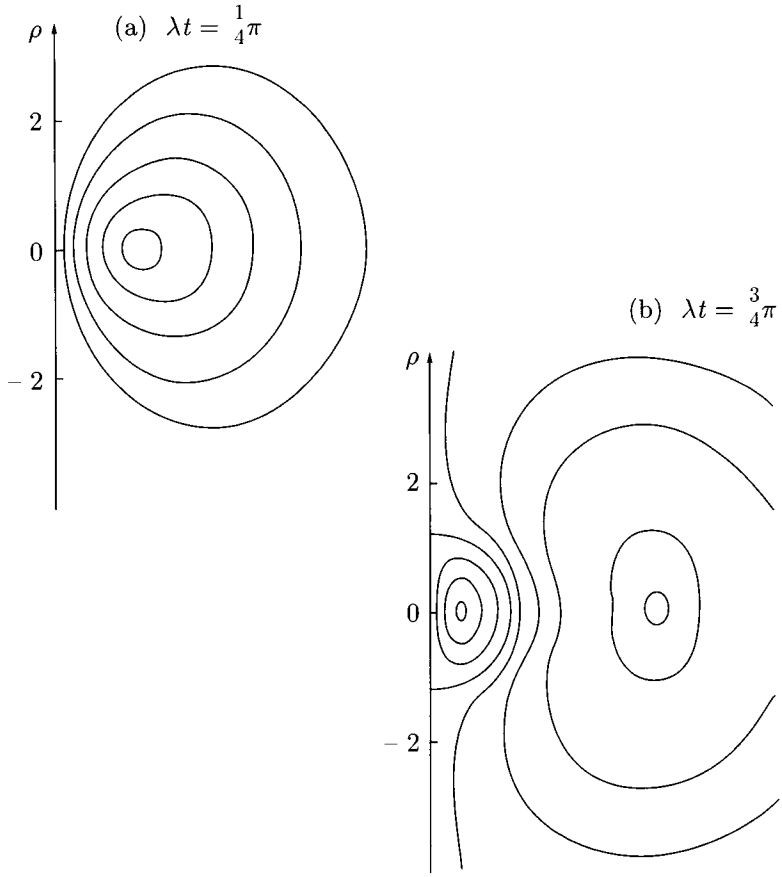

FIG. 7. Streamlines for the flow due to a rotlet outside a circular cylinder in the domain $\rho = O(1)$ for small frequencies λ when $c = 2$: (a) $\lambda t = \frac{1}{4}\pi$; (b) $\lambda t = \frac{3}{4}\pi$.

Finally, in the outermost domain where the $\ln r \cos \lambda t$ term due to the rotlet and the $O(\rho^{-1})$ term in the bracket of (22) balance, we can write the leading terms as

$$\psi \cong \ln r \cos \lambda t + \frac{8 \cos \theta \sin \lambda t}{\pi c \lambda \ln(\lambda^{-1}) r}; \tag{23}$$

the symmetry that existed for $\rho = O(1)$ is no longer present. Therefore, this third region is defined by $\eta = O(1)$ when $\lambda \ll 1$, where

$$\eta = \lambda \ln(\lambda^{-1}) r.$$

The second term in (23) represents a dipole at the origin $\eta = 0$, and the streamlines for

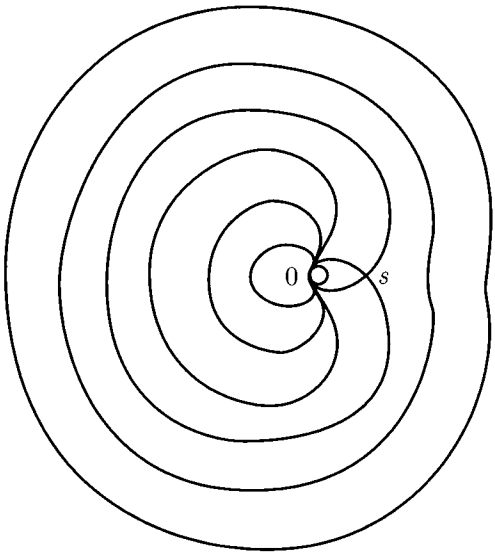

FIG. 8. Streamlines for the flow due to a rotlet and dipole with unit strengths at the origin; this represents the far field flow in the outermost region $\eta = O(1)$ when $\lambda \ll 1$.

a unit rotlet and unit dipole are given in Fig. 8. This pattern is topologically unchanged (except for reflections in the line $|\theta| = \frac{1}{2}\pi$) for all combinations of strengths of the singularities at all times; when the strength of the rotlet is increased, for example, the scale of the diagram as measured by the length of $0S$ is effectively decreased. In the overlap domain where $\rho \to \infty$ and $\eta \to 0$ the dipole dominates. The position of the stagnation point on the axes when $\eta = O(1)$ is represented by $\eta = 4\pi^{-1} \tan \lambda t$ on $\theta = 0$, and $\eta = -4\pi^{-1} \tan \lambda t$ on $\theta = \pi$. Therefore, in this outermost region, the stagnation point moves from infinity to the origin along the axis $\theta = \pi$ during $(n - \frac{1}{2})\pi < \lambda t < n\pi$, and from the origin to infinity along the axis $\theta = 0$ during $n\pi < \lambda t < (n + \frac{1}{2})\pi$ for all integers n. At $\lambda t = n\pi$ the strength of the dipole is zero and the stagnation point S in Fig. 8 has moved to the origin $\eta = 0$; the enclosed region between 0 and S has collapsed. However, it has already been found that there is a symmetry where $\rho = O(1)$ with the stagnation points moving out along both axes $\theta = 0, \pi$. Consequently, it can be conjectured that the point moving out on $\theta = \pi$ when $\rho = O(1)$, and the point moving in when $\eta = O(1)$, coalesce in the overlap region and disappear when $\lambda t \cong 2n\pi$; the free eddy defined by these points has collapsed.

As mentioned earlier, numerical approximations for the situation where $\lambda = 0.01$ have been made, working directly from the formal solution (14). From these, we present the position of the stagnation points on the axes in Fig. 9; the basic features of the results from the asymptotic analysis within each of the three different domains are present. In particular, the conjecture suggested above concerning the collapse of the eddy is confirmed for this example. The asymptotic results for $\rho = O(1)$ are apparent for r very roughly between 8 and 60, where the streamlines are equivalent to those shown in Fig. 7; once r is larger than about 80, Fig. 8 represents the basic pattern.

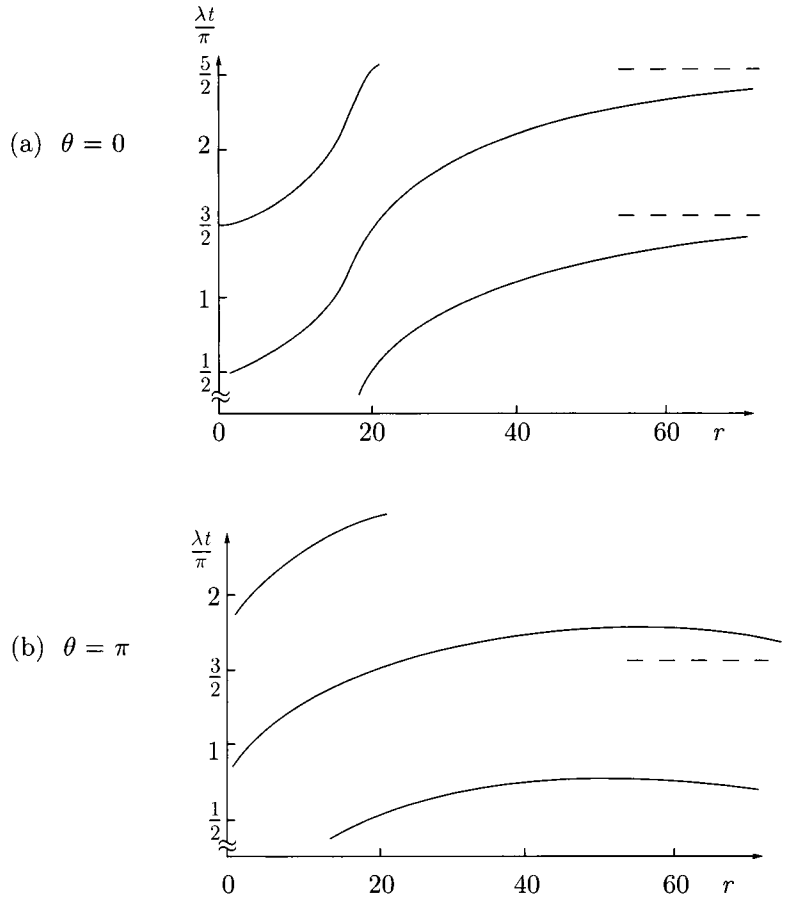

FIG. 9. Position of the stagnation points on the axes (a) $\theta = 0$, (b) $\theta = \pi$ for the flow due to a rotlet at $c = 2$, $\theta = 0$ when $\lambda = 0.01$.

4. Rotlet inside a circular cylinder. To conclude, we consider briefly the bounded situation corresponding to that of the previous section where the rotlet is now inside the cylinder at the point $r = c$, $\theta = 0$ with $0 < c < 1$. The formal solution of Eq. (3) for $0 \leq r \leq 1$, which satisfies the no-slip conditions on $r = 1$, can be developed using an equivalent analysis to that for the exterior case, and the result shows that

$$\Psi = \frac{1}{2}\ln\left\{\frac{r^2 - 2cr\cos\theta + c^2}{1 - 2cr\cos\theta + c^2r^2}\right\} - \sum_{n=0}^{\infty} \frac{\varepsilon_n c^n}{\sigma I_{n+1}(\sigma)}\{I_n(\sigma r) - I_n(\sigma)r^n\}\cos n\theta \qquad (25)$$

where $\varepsilon_0 = 1$, $\varepsilon_n = 2$ for $n = 1, 2, 3, \ldots$; $\sigma^2 = i\lambda$. Consequently, the vorticity on the boundary is given by

$$(\Omega)_{r=1} = -\sum_{n=0}^{\infty} \varepsilon_n c^n \frac{\sigma I_n(\sigma)}{I_{n+1}(\sigma)}\cos n\theta. \qquad (26)$$

In particular, when λ is small, these expressions can be approximated by

$$\Psi = \frac{1}{2}\left[\ln\left\{\frac{r^2 - 2cr\cos\theta + c^2}{1 - 2cr\cos\theta + c^2r^2}\right\} + \frac{(1-r^2)(1-c^2r^2)}{1 - 2cr\cos\theta + c^2r^2}\right] + \frac{i\lambda}{32}(1-r^2)^2\left[1 + \frac{4\cos\theta}{cr} + \frac{2\cos 2\theta}{c^2r^2}\ln(1 - 2cr\cos\theta + c^2r^2) - \frac{4\sin 2\theta}{c^2r^2}\arctan\left(\frac{cr\sin\theta}{1 - cr\cos\theta}\right)\right] + O(\lambda^2) \tag{27}$$

from (25), and

$$(\Omega)_{r=1} = -2\frac{(1 - 4c^2 - c^4) + 4c^3\cos\theta}{(1 - 2c\cos\theta + c^2)^2} + \frac{i\lambda}{4}\left[1 + \frac{4\cos\theta}{c} + \frac{2\cos 2\theta}{c^2}\ln(1 - 2c\cos\theta + c^2) - \frac{4\sin 2\theta}{c^2}\arctan\left(\frac{c\sin\theta}{1 - c\cos\theta}\right)\right] + O(\lambda^2) \tag{28}$$

from (26). The $O(1)$ solution in (27) describes the steady-state motion, with the $O(1)$ vorticity in (28) showing separation on the boundary at $|\theta| = \theta_a$, where $\cos\theta_a = (c^4 + 4c^2 - 1)/(4c^3)$, for all $c > \sqrt{2} - 1$ (cf. Wannier [12], Ranger [13]). The expressions (27) and (28) represent regular perturbations in λ, thereby indicating that an alternate approach is possible when λ is small: we can write the solution of (3) as a series $\Psi(r, \theta; \lambda) = \sum_{m=0}^{\infty} \lambda^m \Psi_m(r, \theta)$, where Ψ_0 is the steady-state solution, and then proceed to solve iteratively for Ψ_m, $m = 1, 2, 3, \ldots$. A well-defined boundary-value problem exists at each stage in the process, leading to unique solutions Ψ_m. Because it is found that the magnitudes of the contributions Ψ_m decrease fairly rapidly as m increases, few terms are required for even moderate values of λ; in fact, two decimal place accuracy is possible from just three terms (i.e., including $O(\lambda^2)$) when λ is equal to unity. A physical consequence is that the transition is rapid.

The motion is quasi-steady with the physical stream function $\psi(r, \theta, t)$ given by $\Psi_0(r, \theta)\cos\lambda t$ for all times t except for those around $\lambda t = \frac{1}{2}\pi$ where $\cos\lambda t = O(\lambda)$, which is equivalent to $\lambda t = \frac{1}{2}\pi + O(\lambda)$ (when we consider $0 \leq \lambda t \leq \pi$ only). We now consider the nature of this transition. The numerical results are presented for $\lambda = 0.1$, which is found to be sufficiently small for the terms given in (27) and (28) to give accuracy in the streamline patterns at each stage. We set $c = \frac{2}{3}$.

The streamlines for $t = 0$ are shown in Fig. 10(a), with separation points at $|\theta_s| \cong 34.6°$, and little change is observed as the strength of the rotlet decreases until $0.1t$ is approximately 0.48π, when the separation points still show $|\theta_s(t)| > 31°$. Subsequently, the region occupied by the counter-rotating eddy expands (Fig. 10(b)). At $0.1t = 0.4993\pi$ the separation points have moved to $\theta = 0$ where they vanish; for $0.4993\pi < 0.1t < \frac{1}{2}\pi$ there is a second stagnation on the axis as the closed cell about the rotlet continues to collapse (Fig. 10(c)). At $0.1t = \frac{1}{2}\pi$, when the strength of the rotlet is zero, this cell vanishes (Fig. 10(d)), to reappear on the other side in a continuous process, with the separate free eddy as the remnant of the counter-rotating eddy present for $0.1t < \frac{1}{2}\pi$

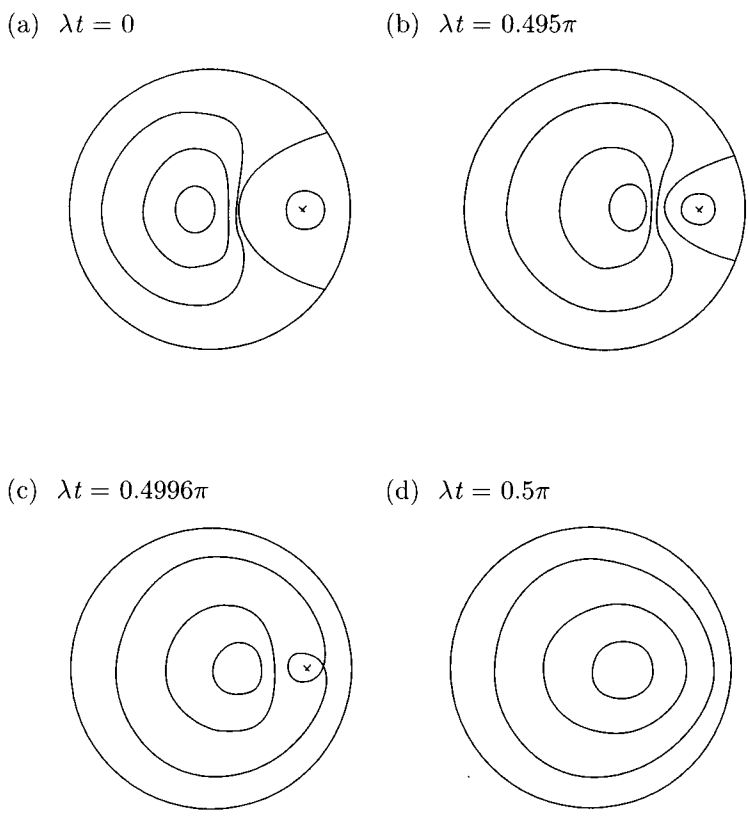

FIG. 10(i). Streamlines for the flow due to a rotlet inside a circular cylinder when $c = \frac{2}{3}$, $\lambda = 0.1$: (a) $\lambda t = 0$; (b) $\lambda t = 0.495\pi$; (c) $\lambda t = 0.4996\pi$; (d) $\lambda t = 0.5\pi$.

(Fig. 10(e)). This free eddy disappears when $0.1t = 0.5004\pi$ as the two stagnation points coalesce; at this stage, just the simple weak, rotating flow remains (Fig. 10(f)). However, when $0.1t = 0.5056\pi$ this weak flow separates at $|\theta| \cong 103.1°$, and two attached eddies grow very quickly around the boundary (Fig. 10(g)), becoming a single eddy as the two separation points coincide at $\theta = \pi$ when $0.1t = 0.5057\pi$. This single eddy proceeds to grow (Fig. 10(h)); when $0.1t$ is about 0.52π the streamlines have essentially returned to the quasi-steady pattern given in Fig. 10(a), as the separation points then show $|\theta_s| < 39°$, and the transition is basically complete.

In general, when λ is small enough that only the terms in (27) are required to give numerical accuracy, the corresponding transition occupies times t such that $(\frac{1}{2} - 0.2\lambda)\pi < \lambda t < (\frac{1}{2} + 0.2\lambda)\pi$; the total time is therefore independent of λ.

The process described so far is relevant for all positions of the rotlet on the axis where $c > \frac{1}{2}$. If $\sqrt{2} - 1 < c < \frac{1}{2}$ the only change is that in the later stages the separation in the weak rotating flow takes place at $\theta = \pi$, and so the motion represented by Fig. 10(g) is absent; there is a direct transition from the flow sketched in Fig. 10(f) to the single eddy pictured in Fig. 10(h).

(e) $\lambda t = 0.5002\pi$ (f) $\lambda t = 0.502\pi$

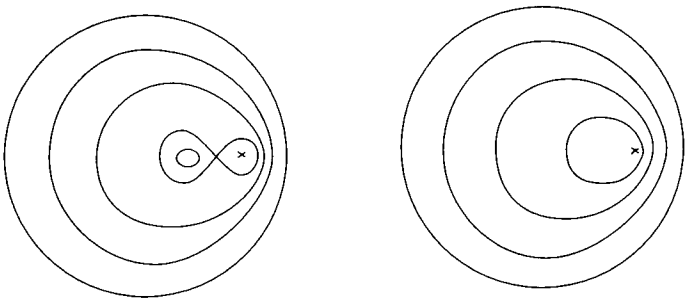

(g) $\lambda t = 0.5056\pi$ (h) $\lambda t = 0.51\pi$

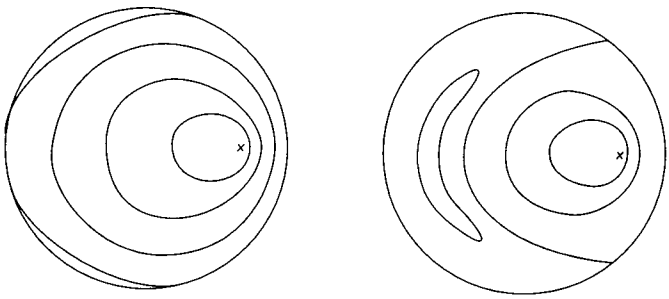

FIG. 10(ii). Streamlines for the flow due to a rotlet inside a circular cylinder when $c = \frac{2}{3}$, $\lambda = 0.1$: (e) $\lambda t = 0.5002\pi$; (f) $\lambda t = 0.502\pi$; (g) $\lambda t = 0.5056\pi$; (h) $\lambda t = 0.51\pi$.

When $c < \sqrt{2} - 1$ there is no separated region in the steady-state motion, and so none for the quasi-steady flow either. The particular case $c = \frac{1}{3}$, and $\lambda = 0.1$, has been considered numerically with the following conclusions: as the strength of the rotlet decreases it is not until the time t given by $0.1t \cong 0.4844\pi$ that separation occurs at $\theta = \pi$, and an eddy with counter-rotating fluid develops; the streamlines are equivalent (topologically) to Figs. 10(a) or (b). The pattern then proceeds to follow that presented for $c = \frac{2}{3}$: (i) the separation points move around the boundary to $\theta = 0$, reaching there at $0.1t = 0.4985\pi$, (ii) the stage shown in Fig. 10(c) occupies $0.4985\pi < t < \frac{1}{2}\pi$, and (iii) the stage shown in Fig. 10(e) occupies $\frac{1}{2}\pi < 0.1t < 0.5002\pi$. Subsequently, there is a single cell again, and there are not further changes until the next transition when $0.1t$ is close to $\frac{3}{2}\pi$. When $c = \frac{1}{3}$, the total transition occupies the time $(\frac{1}{2} - 0.156\lambda)\pi < \lambda t < (\frac{1}{2} + 0.002\lambda)\pi$ for all λ small enough that (27) adequately represents the behaviour.

The author wishes to thank the Natural Sciences and Engineering Research Council of Canada for a grant-in-aid of research during the time this work was completed.

Appendix. A vector invariant form of solution. By H. A. Stone, Division of Applied Sciences, Harvard University. Here we present a vector invariant argument to obtain the solution for the oscillatory flow past the circular cylinder $r = 1$, which was considered in Sec. 2.

In dimensional coordinates it is necessary to solve $\mathbf{u}_t = -\boldsymbol{\nabla} P + \nabla^2 \mathbf{u}$, plus $\boldsymbol{\nabla} \cdot \mathbf{u} = 0$ for the velocity vector $\mathbf{u}$ and pressure P, with $\mathbf{u} \to \mathbf{V} e^{i\lambda t}$ as $|\mathbf{r}| \to \infty$ and $\mathbf{u} = \mathbf{0}$ on $|\mathbf{r}| = 1$. The time-dependence is removed by first letting $\mathbf{u} = e^{i\lambda t}\mathbf{v}$ and $P = e^{i\lambda t} p$, for

$$i\lambda \mathbf{v} = -\boldsymbol{\nabla} p + \nabla^2 \mathbf{v} \quad \text{plus} \quad \boldsymbol{\nabla} \cdot \mathbf{v} = 0. \tag{A.1}$$

Now $\mathbf{v}$ can be decomposed into homogeneous and particular solutions by $\mathbf{v} = \mathbf{v}_h + \mathbf{v}_p$ where

$$\nabla^2 \mathbf{v}_h = i\lambda \mathbf{v}_h \quad \text{and} \quad \mathbf{v}_p = i\lambda^{-1} \boldsymbol{\nabla} p; \tag{A.2}$$

also, we must have $\nabla^2 p = 0$ from (A.1).

A vector representation can be constructed through taking $p = -i\lambda \mathbf{V} \cdot \mathbf{r} + \alpha r^{-2} \mathbf{V} \cdot \mathbf{r}$, for some constant α, which shows

$$\mathbf{v}_p = \mathbf{V} + \frac{i\alpha}{\lambda} \left\{ \frac{\mathbf{V}}{r^2} - \frac{2\mathbf{V} \cdot \mathbf{rr}}{r^4} \right\}. \tag{A.3}$$

Further, a solution for $\mathbf{v}_h$ has the form

$$\mathbf{v}_h = \beta \mathbf{V} K_0(\sigma r) + \gamma \mathbf{V} \cdot \boldsymbol{\nabla} \{ \boldsymbol{\nabla} K_0(\sigma r) \}, \tag{A.4}$$

where $\sigma = (i\lambda)^{\frac{1}{2}}$ and, from continuity, the constants β and γ are connected by $\beta = -i\lambda\gamma$. When (A.3) and (A.4) (after some simplification) are combined, it follows that

$$\begin{aligned} \mathbf{v} = \mathbf{V} + \frac{i\alpha}{\lambda} \left\{ \frac{\mathbf{V}}{r^2} - \frac{2\mathbf{V} \cdot \mathbf{rr}}{r^4} \right\} - \gamma \Bigg[\sigma K_1(\sigma r) \left\{ \frac{\mathbf{V}}{r} - \frac{2\mathbf{V} \cdot \mathbf{rr}}{r^2} \right\} \\ - \sigma^2 K_0(\sigma r) \left\{ \frac{\mathbf{V}}{r} - \frac{\mathbf{V} \cdot \mathbf{rr}}{r^2} \right\} \Bigg], \end{aligned} \tag{A.5}$$

and applying the boundary conditions shows that

$$\alpha = -\{2\sigma K_1(\sigma) + \sigma^2 K_0(\sigma)\}/K_0(\sigma), \qquad \gamma = \frac{-2i}{\lambda K_0(\sigma)}, \tag{A.6}$$

to complete the solution. Finally, the vorticity $\boldsymbol{\omega} = \boldsymbol{\nabla} \times \mathbf{u}$ is given by

$$\boldsymbol{\omega} = \frac{2\sigma K_1(\sigma r)}{K_0(\sigma)} \frac{\mathbf{V} \times \mathbf{r}}{r} e^{i\lambda t}, \tag{A.7}$$

which coincides with the result of Sec. 2.

References

[1] G. G. Stokes, *On the effect of the internal friction of fluids on the motion of a pendulum*, Trans. Cambridge Philos. Soc. **9**, 9–106 (1851)

[2] C. W. Oseen, *Über die Stokessche Formel und über eine verwandt Aufgabe in der Hydrodynamik*, Ark. Mat. Astr. Fys. **6**, no. 29 (1910)

[3] S. Kaplun and P. A. Lagerstrom, *Asymptotic expansion of Navier-Stokes solutions for small Reynolds numbers*, J. Math. Mech. **6**, 585–593 (1957)

[4] I. Proudman and J. R. A. Pearson, *Expansions at small Reynolds numbers for the flow past a sphere and a circular cylinder*, J. Fluid Mech. **2**, 237–262 (1957)

[5] G. B. Jeffery, *The rotation of two circular cylinders in a viscous fluid*, Proc. Roy. Soc. (A) **101**, 169–174 (1922)

[6] S. Tomotika and T. Aoi, *The steady flow of viscous fluid past a sphere and circular cylinder at small Reynolds numbers*, Quart. J. Mech. Appl. Math. **3**, 140–161 (1950)

[7] J. M. Dorrepaal, M. E. O'Neill, and K. B. Ranger, *Two-dimensional Stokes flows with cylinders and line singularities*, Mathematika **31**, 65–75 (1984)

[8] C. Pozrikidis, *A study of linearized oscillatory flow past particles by the boundary-integral method*, J. Fluid Mech. **202**, 17–41 (1989)

[9] S. Kim and S. J. Karrila, *Microhydrodynamics*, Butterworth-Heinemann, Boston, 1991

[10] A. B. Basset, *A treatise on hydrodynamics*, Vol. 2, Deighton Bell, Cambridge, 1888

[11] M. Abramowitz and I. A. Stegun, *Handbook of Mathematical Functions with Formulas, Graphs, and Mathematical Tables*, Dover Publications, New York, 1965

[12] G. Wannier, *A contribution to the hydrodynamics of lubrication*, Quart. Appl. Math. **8**, 1–32 (1950)

[13] K. B. Ranger, *Eddies in two dimensional Stokes flow*, Internat. J. Engrg. Sci. **18**, 181–190 (1980)